Design of an apparatus to measure the shear response of ultrathin liquid films

James Peachey, John Van Alsten,[a] and Steve Granick
Materials Research Laboratory, University of Illinois, 104 South Goodwin, Urbana, Illinois 61801

(Received 20 August 1990; accepted for publication 3 October 1990)

The design, calibration, and performance are described of an apparatus to study the shear response of ultrathin liquid films. The device, a modification of the surface forces apparatus, measures the resistance to shear of liquids confined between two atomically smooth solid surfaces. The surfaces are separated by distances on the order of the size of the liquid molecules (liquid film thickness < 10 nm). Shear forces with periodic time dependence are applied to one surface while the second is held fixed, and any motion so induced is analyzed to determine the behavior of the liquid film. The frequency and amplitude of the shear forces applied can be varied over a wide range (0.03–60 Hz frequency and 0.1–1000 nm amplitude) to achieve different values for the magnitude of the shear rate. The dynamic response of the device is linear in the applied force at a given frequency; nonetheless, nonlinear dependence of the liquid's shear resistance on the shear rate, net normal pressure, and film thickness can be observed with the technique. The mechanical and electrical characteristics of the device are modeled to gain insight into its behavior and facilitate analysis of the measured data. The central results of this approach are expressions for the magnitude of the shear rate and an effective friction coefficient of the liquid film in terms of easily measured electrical quantities. For convenience the friction coefficient is restated as an apparent dynamic viscosity in analogy to continuum hydrodynamics, but the validity of the approach does not depend on a particular understanding of the structure in the liquid layer. The applications and limitations of the device are discussed, as well as other potential uses to which the apparatus may be applied by rational extension to the approach presented.

I. INTRODUCTION

In recent years, interest in thin liquid films has grown due to the varied and complex behavior they display. One area that still lacks sufficient fundamental understanding is the dynamics of shear flow in constricted geometries. Some questions of relevance are how does the interaction of the surface with the liquid affect shear flow? Which aspects of the behavior of thin liquid films can be attributed to the confinement alone? What is the thermodynamic nature of states in which a thin film may exist? Under what conditions, if any, does such a film behave like a continuous fluid? Such issues are difficult to address experimentally, not only because of the delicate nature of the phenomena, but because it is difficult to implement experiments that admit unambiguous interpretation. In order to obtain measurements whose essential physical meaning is clear, the development and precise characterization of new instruments is desirable.

In the present context, what is desired is a device that can create a thin liquid film by bringing very close together two surfaces in contact with a reservoir of bulk liquid. The device must be capable of applying shear forces to one of the surfaces, and measuring the amplitude of any resulting motion of that surface, thereby obtaining information about how the liquid responds to being sheared. The design is tempered by the size of the quantities involved. The shear displacements that must be measured are typically found to be on the order of nanometers when the applied shear forces are on the order of microNewtons. Moreover, the film thickness should be on the order of the size of the molecules under study in order to induce interesting thin-film effects; surface separations between a few and a few hundred Angstroms should be measurable with high precision.

It is desirable to use surfaces that are flat, parallel, and atomically smooth, to eliminate as much as possible surface roughness and film inhomogeneities parallel to the surfaces. Smoothness on the atomic scale traditionally has been achieved by making the surfaces out of mica, which can be cleaved step-free on the scale of square centimeters. Recently it has also become possible to create self-assembled monolayers of short chains that bind chemically to the mica at one end and present at the other an end-group with any desired chemical functionality.[1,2] The resulting surface has the smoothness of the mica, but a surface chemistry of the experimenter's choosing, thus greatly expanding the variety of systems which can potentially be explored. All shear results referred to in this article were obtained with bare mica.

In Fig. 1 is shown a shear device that was designed with the above considerations in mind. Precise measure-

[a]Current address: Central Research and Development, Dupont Experimental Station, Wilmington, DE 19880.

 0034-6748/91/020463-11$02.00

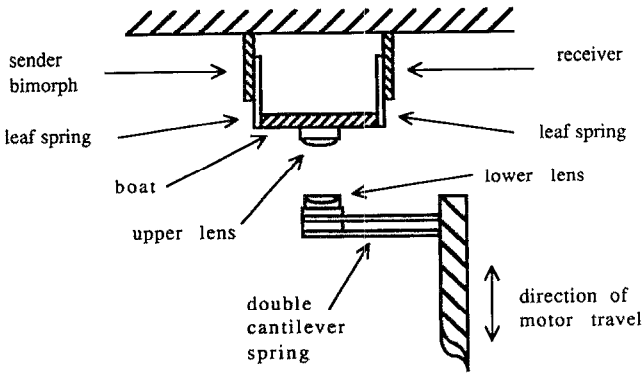

FIG. 1. A schematic drawing of the shear apparatus. The surface separation is controlled and measured in the same way as in a surface forces device. The shear force is generated by the left-hand piezoelectric bimorph (the "sender"), and the response of the device induces a voltage across the right-hand bimorph (the "receiver"). The leaf springs are included to increase the elastic response of the device.

ment and control of the fine shear motions and forces is accomplished through the use of electromechanical transducers (piezoelectric bimorphs), which permit detailed information about the mechanical responses of the liquid to be gathered with the ease of simple electrical measurements. Shear forces are created by applying an electrical signal to one of the transducers, and any resulting motion of the surface induces an electrical signal in a second transducer. Measurements of these two signals can be analyzed to reveal the response of the liquid to the shearing surface.

Previously we have described results obtained with the device for some simple liquids and two siloxane homopolymers.[3–9] Two qualitatively different electrical output waveforms were observed, indicating two physically different responses of the liquid film. The first type of response is identified by output signals that increase monotonically with the magnitude of the (sinusoidal) input signals, and occur at the same frequency, which implies that the liquid responds linearly to the driving force. In this regard, the behavior is similar to what one would expect from a viscous fluid. Because of this similarity, and since the structure of the liquid film is not completely understood at present, this behavior is analyzed by calculating from the signals an apparent dynamic viscosity using continuum hydrodynamics.

To calibrate away the characteristic response of the device itself, the apparent viscosity is calculated from a comparison of the output signal observed with liquid between the surfaces to the output signal observed with the surfaces completely separated [see Fig. 2(a)]. (The expression used to calculate the apparent viscosity is derived below.) In every liquid studied, the observed apparent dynamic viscosity in thin films was many orders of magnitude greater than that of the bulk liquid, and exhibited marked nonlinear dependence on film thickness, shear rate and net normal pressure.[3,8,9] These differences from classical fluid behavior make it clear that the continuum description does not capture the true nature of the film. Nonetheless, the

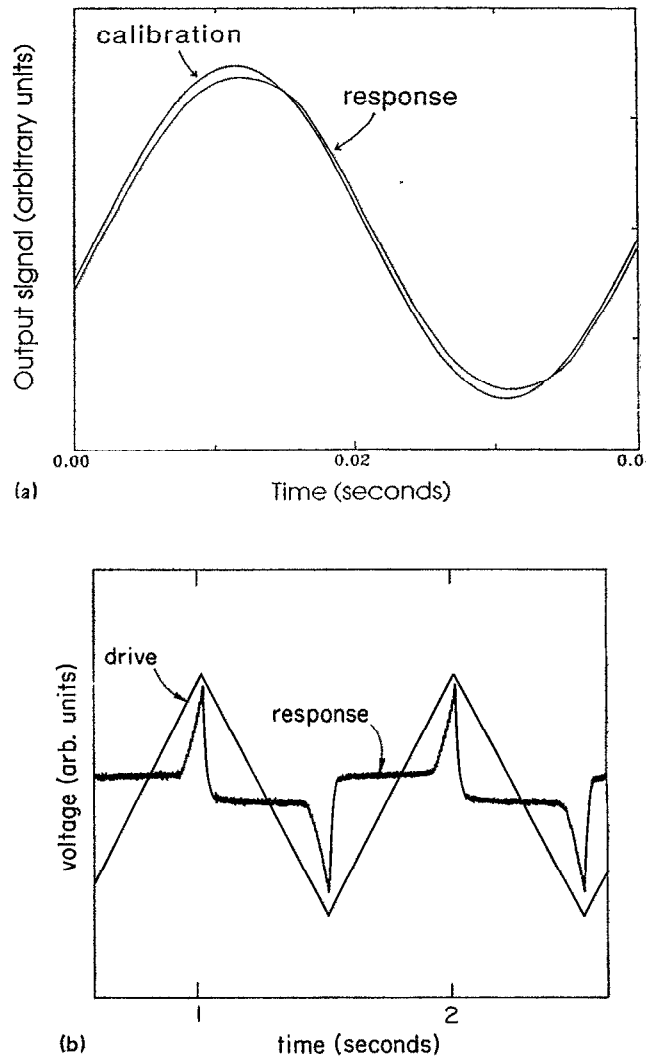

FIG. 2. (a) Two output signals induced by an applied sine wave (not shown) are displayed. The "calibration" waveform is obtained with the mica sheets completely separated. The "response" waveform is obtained with a thin liquid film between the sheets, which causes it to lag the calibration waveform. This phase lag can be analyzed to yield the apparent dynamic viscosity of the liquid film. (b) These waveforms typify the yield stress behavior. The "excitation" waveform induces a proportional shear stress on the liquid film. The "response" waveform remains very small, indicating that the surfaces are stuck together, until the applied stress reaches a yield point. At this yield point the slope of the response waveform increases dramatically, indicating the onset of sliding.

apparent dynamic viscosity is a useful way to report the data, precisely because it shows these differences so strikingly.

The second type of response, shown in Fig. 2(b), calls at the outset for other means of interpretation. In this case, the output waveform is not linear in the input (triangular) waveform, but remains nearly zero up to a point, then responds linearly for a time before again "sticking" upon returning to zero. This implies that the surfaces do not slide past each other until a yield stress is exceeded, a response which suggests that the film behaves more like a solid than a liquid on the time scale of the experiment.[7,8] There is a small but nonzero electrical response observed

during the "stick," which may be attributed to the compliance of the adhesive used to bind the mica to the lenses. Potential effects of the compliance of the adhesive are discussed in the Appendix.

It should be clear from these results that in order to infer properly the behavior of the liquid from the measured electrical signals, it is necessary to understand in detail the workings of the shear device itself. This has been accomplished through the development of a model of the device that accurately describes its behavior. The purpose of the present article is to describe this model, and show how it leads to a method of data analysis that does not rely on a particular model of the liquid film.

II. DESCRIPTION OF THE SHEAR DEVICE

The creation of the film, measurement of its thickness, and general spirit of the technique are well accommodated by the surface forces apparatus,[10,11] so the device design resembles the surface forces apparatus in many respects. A simple way to obtain parallel-plate geometry is to mount the mica sheets on cylindrical quartz lenses, and bring them together in a crossed cylinder configuration. If the adhesive used to mount the mica is sufficiently compliant, the mica will flatten under the action of adhesive forces or normal load to produce a "region of contact," in which the surfaces are locally planar and parallel. This region of contact is considered to be the area of the thin film because outside this region the separation of the surfaces rapidly increases, so the liquid outside the region of contact is effectively in a bulk state and makes a negligible contribution to the overall response observed.

The adhesive used to mount the mica may vary depending on the application, but it should be sufficiently compliant to allow this flattening to occur. Two adhesives used in the past are (1,5)diphenylcarbazide, and a mixture of equal portions of galactose and fructose, the former of which results in quite stiff, the latter in more compliant bonding. As mentioned in the Introduction, the compliance of the glue is responsible for the (very slight) motion of the surface that occurs before the onset of slipping in the yield stress response. The compliance of the adhesive could in principle allow the shape and location of the flattened region to change when the surfaces are sheared, thus affecting the results obtained. In practice, this is not a difficulty, since the lateral displacements used are less than 1% of the diameter of contact, and over such small displacements the rheology of the adhesive may be considered essentially fixed. The effects of the adhesive on the experiment are discussed more thoroughly in the Appendix.

The contact area and film thickness can be determined using multiple beam interferometry between silver films on the back sides of the mounted sheets, just as in a conventional surface forces apparatus[12] (see Fig. 3). The drive mechanism for controlling the position of the surfaces is the same as the one previously described.[13]

This is where the similarity between the shear device and the surface forces apparatus ends. The device features a modification for the purpose of creating and measuring shear, which is shown in detail in Fig. 1. The bottom lens

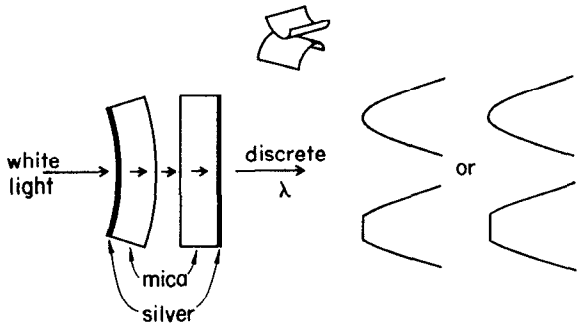

FIG. 3. The interference of white light passing through the mica sheets allows only a discrete set of wavelengths to penetrate. These are observed as a set of interference fringes, whose wavelengths are determined by the thickness of the mica sheets, the distance between them and the refractive indices of all components in the optical path. The difference of the fringe position when liquid is present from that when the surfaces are in adhesive contact (zero separation) yields the film thickness with a resolution of ±0.1 nm. When crossed cylinders deform, they produce a locally flat, parallel area of contact. This flattening can be observed in the shape of the interference fringes.

is held stationary, while the top lens is held in a rectangular "boat," which is suspended from the upper portion of the apparatus by a piezoelectric bimorph at each end. (The leaf springs appearing in Fig. 1 will be explained below.) A bimorph is a thin, rectangular slab made by layering two sheets of piezoelectric material poled in opposite directions, so that a voltage applied across the two sides of the bimorph causes its tip to bend owing to the expansion of one sheet and contraction of the other.[14] Conversely, if a bimorph is bent a voltage is produced. Thus, the shear force in the present device is created by applying an input voltage across one of the bimorphs (the "sender"). Any response of the device induces an output voltage across the other bimorph (the "receiver"), which can be easily measured, e.g., on an oscilloscope.

The reason for using a piezoelectric bimorph to produce the shear force is that it is easy to adjust the input voltage to produce forces of the desired magnitude. Similarly, while the resulting displacements of the boat are far too small to be observed optically, they are sufficient to induce a measurable output voltage across the receiver bimorph. Thus, the use of bimorphs meets the design specifications, allowing sensitive access to subtle phenomena. This design is also flexible because it is possible, simply by changing the waveform of the input electrical signal, to induce time-varying stresses with different characteristic wave shapes. For example, when studying "viscous" behavior, like that shown in Fig. 2(a), it is convenient for the calculation of the apparent viscosity to use a sine wave input. On the other hand, to observe yield stress behavior it is desirable to ramp the stress up past the yield point at a constant rate; hence a triangular waveform is applied for these measurements [see Fig. 2(b)].

The other components in the device that warrant further explanation are the leaf springs between the bimorphs and the boat. There are several reasons to include these springs. One is that it would be difficult as a practical

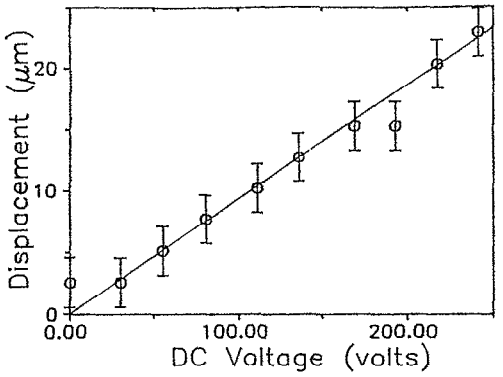

FIG. 4. The displacement of the boat measured optically as a function of dc voltage applied. Typically, the response of the device is linear for dc voltages under 300 V. The upper voltage limit of this linear region decreases with increasing frequency, generally (depending on the device) dropping as low as ~80–100 V at 100 Hz.

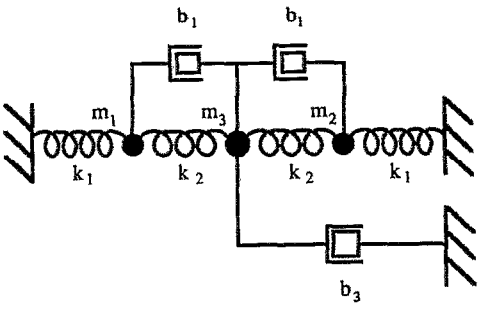

FIG. 6. The mechanical model for the device shown in Fig. 1. A force proportional to the input voltage acts on the leftmost mass (m_1). The output voltage is determined by the motion of the rightmost mass (m_2) and can be analyzed to determine how the device is responding to the input voltage. The presence of the liquid film is modeled by the lower dashpot (friction coefficient b_3), which exerts a frictional force on the central mass m_3.

matter to attach the bimorphs directly to the boat. Even if this could be performed, the resulting device would be extremely delicate, as the bimorphs are very brittle. Another reason is that the bimorphs are so stiff that the system would be extremely damped and the output voltages unmeasurably small. The leaf springs act to increase the elastic response of the device.

Although the shear apparatus is ultimately operated using small input voltages ($V_1 \leqslant 1$ V), it is possible to observe the motion of the boat optically only if the input voltage is much higher ($V_1 \geqslant 100$ V). The displacement induced is linear in the dc voltage applied over a large interval of higher voltages (see Fig. 4). Similarly, displacement is linear if a static mechanical force is applied. When weights are hung from the bimorph assembly the resulting displacement is proportional to the force, up through much larger displacements than those normally used in experiments (see Fig. 5). Since nonlinearities would be expected to occur, if at all, at large displacements, it is reasonable to assume that the displacement is linear in both static force and dc voltage throughout the normal region of device operation. This assumption underlies the development of the model to be described.

The rest of this article is devoted to explaining how the input and output voltages can be used to determine the apparent viscosity of the confined liquid, and the magnitude of the velocity and shear rate of the motion, *without* direct measurement of the boat displacement. First, a model of the instrument is presented that captures the essence of its behavior. As the bimorphs are electromechanical in nature, the model has a mechanical aspect and an electrical one, which are discussed separately. The mathematics of the model are then solved, and compared directly to experimental calibrations of the device. Next the results of the model are used to obtain expressions for the apparent dynamic viscosity and the shear rate. We conclude by describing the calibrations and limitations of the device, and prospects for extending its usage to a larger range of frequencies as well as investigations of other phenomena, such as the shear behavior of confined viscoelastic liquids.

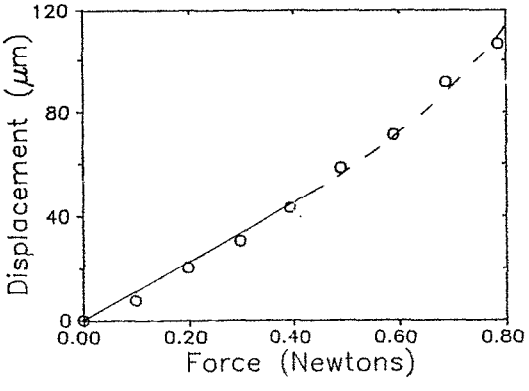

FIG. 5. The displacement of the boat measured optically as a function of applied static force. The response is linear for applied forces less than 0.50 N, which is much larger than the forces present in a typical experiment.

III. THE MECHANICAL MODEL

It is useful to motivate the analysis before becoming specific. The idea of the mechanical model is to replace the device with a combination of effective masses, springs and dashpots, as shown in Fig. 6. More will be said in justification of this simple, linear model, but for the moment the validity of this approach should at least seem plausible in view of the linear response described in the Introduction. The piezoelectric stress from the sender bimorph enters the model as an "external force" which acts on the leftmost mass. Any resulting movement of the rightmost mass induces an output voltage, which so far as the mechanical model is concerned, is another external force. Applying Newton's laws immediately leads to a complete specification of the boat displacement as a function of the external forces, i.e., the voltages.

Within the model, the friction due to the liquid layer is a parameter which could in principle be determined from this expression by measuring independently the displacement and the voltages. But since the displacements desired for normal device operation are too small to be measured directly, all the information sought about the liquid must come from the input and output voltages alone (this is actually the reason for employing piezoelectric bimorphs in the first place). Therefore, while knowing the displacement as a function of the voltages is useful in understanding the behavior of the device, it alone does not yield the quantities of interest. After the model has been explained and solved, it will therefore be necessary to make an approximation to determine the apparent viscosity and shear rate from the electrical signals.

Now the mechanical model will be explored in detail. The first step is to understand how the bimorphs transduce forces and voltages. The microscopic equations of piezoelectricity, in a linear medium, are[14]

$$S = Y\sigma + c_1 E, \tag{1a}$$

$$D = \varepsilon E + c_2 S, \tag{1b}$$

where S, σ, and Y are the stress, strain, and Young's modulus, respectively, and D, ε, and E are the electric displacement, dielectric constant, and electric field, respectively. The coefficients c_1 and c_2 are coupling constants that give rise to the piezoelectric effect. In the case $c_1 = c_2 = 0$ the Eqs. (1) reduce to the usual linear relations between S and σ, and between D and E, respectively.

Equations (1) apply at each point in the bimorph. Integration of these equations over the volume of the bimorph results in a force law which has a Hookean spring term, plus an extra term describing the presence of the piezoelectric stress.[14] This latter term is proportional to the voltage because the electric field has been effectively integrated along a path between the charge bearing surfaces of the bimorph. Thus, for small displacements and voltages, the total force law of the bimorphs may be written:

$$F_{1,\mathrm{TOT}} = -k_1 x_1 + f(V_1) \quad \text{(sender)}, \tag{2a}$$

$$F_{2,\mathrm{TOT}} = -k_1 x_2 + f(V_2) \quad \text{(receiver)}, \tag{2b}$$

where $f(V) \equiv \Gamma V$ is a force proportional to the voltage V across the bimorph, x_1 and x_2 are the horizontal deflections of the bottoms of the sender and receiver bimorphs, respectively, and k_1 is the spring constant of the bimorphs. It should be noted that each bimorph behaves exactly like a forced spring, which justifies the use of the model depicted in Fig. 6. The limit of "small voltage" will be stated more precisely later.

The next step is to calculate the response of the mechanical model to this force. The two outer springs represent the intrinsic mechanical stiffness of the bimorphs and are given the spring constant k_1 introduced above. The inner springs, with spring constant k_2, represent the leaf springs. As explained in the Introduction, $k_2 \ll k_1$. The masses m_1 and m_2 are lumped equivalent masses, representing the effective masses of the bimorph-leaf spring combinations. The third mass, m_3, is mainly the mass of the boat, lens and mica. It is assumed that the masses m_1 and m_2 are equal, just as above the assumption was tacitly made that both bimorphs and both leaf springs have the same spring constants.

There are two sources of dissipation (friction) in the system. The first is the intrinsic friction of the device itself. It is reasonable to assume that most of this is caused by the adhesive that holds the bimorphs to their leaf springs. This intrinsic friction is represented by dashpots appearing between m_3 and the other two masses, as shown in Fig. 6. The frictional forces these dashpots exert are proportional to the relative velocities between the boat and the two effective masses. The displacements of the masses m_1, m_2, m_3 from their equilibrium positions will be denoted by x_1, x_2, x_3, respectively. The frictional force due to the device on, for example, m_1, will be

$$f_{\mathrm{device}} = -b_1(\dot{x}_1 - \dot{x}_3), \tag{3}$$

where b_1 is the intrinsic friction coefficient of the device.

The second source of friction is the presence of liquid between the sheets, and is represented by a third dashpot between the central mass and the wall of the apparatus. The resulting force acts on m_3 alone, and is proportional to its velocity:

$$f_{\mathrm{liquid}} = -b_3(\dot{x}_3), \tag{4}$$

where b_3 is the (unknown) friction coefficient of the liquid. The coefficient b_3 can be related directly to the apparent viscosity of the confined fluid, a quantity of interest. Therefore, one goal of this analysis is to calculate b_3 from the measurable quantities, namely the voltages and their relative phases. In order to do this, it will be necessary first to obtain an expression for the gain $a \equiv V_2/V_1$ as a function of frequency and the parameters b_1, b_3, k_1, k_2, $m_1 = m_2$, and m_3 introduced above, but with all dependence on the unmeasurable coordinates x_j removed. This has the additional benefit of facilitating comparison of the model to the observed behavior of the device.

Now that all the forces present in the system are understood, it is straightforward to write down Newton's equations for the mechanical model shown in Fig. 6. The result is

$$m_1\ddot{x}_1 = -k_2(x_1 - x_3) - k_1 x_1 - b_1(\dot{x}_1 - \dot{x}_3) + f_1(t), \tag{5a}$$

$$m_2\ddot{x}_2 = -k_2(x_2 - x_3) - k_1 x_2 - b_1(\dot{x}_2 - \dot{x}_3) + f_2(t), \tag{5b}$$

$$m_3\ddot{x}_3 = -k_2(x_3 - x_1) - k_2(x_3 - x_2) - b_1(\dot{x}_3 - \dot{x}_1) - b_1(\dot{x}_3 - \dot{x}_2) - b_3\dot{x}_3 \tag{5c}$$

where $f_1(t)$ is the "driving force," proportional to the (applied) sender bimorph voltage, and $f_2(t)$ is the "response force," proportional to the (measured) receiver bimorph voltage.

The problem is now simply that of a damped and driven set of coupled harmonic oscillators. We next consider the case in which the applied voltage is oscillatory,

with frequency ω. Then the forced solution may be obtained using complex notation by writing:

$$x_j(t) \equiv X_j e^{(i\omega t)}, \tag{6a}$$

$$f_j(t) \equiv m_j F_j e^{(i\omega t)}, \tag{6b}$$

for each coordinate $x_j(t)$, $j = 1,2,3$ and each force $f_j(t)$, $j = 1,2$. Here $i \equiv \sqrt{-1}$ and the variables X_j and F_j are complex, giving both the amplitude and relative phase of the variables. Substituting Eqs. (6) into Eqs. (5) results in

$$-m_1\omega^2 X_1 = -k_2(X_1 - X_3) - k_1 X_1 - i\omega b_1(X_1 - X_3) + m_1 F_1, \tag{7a}$$

$$-m_2\omega^2 X_2 = -k_2(X_2 - X_3) - k_1 X_2 - i\omega b_1(X_2 - X_3) + m_2 F_2, \tag{7b}$$

$$-m_3\omega^2 X_3 = -k_2(X_3 - X_1) - k_2(X_3 - X_2) - i\omega b_1(X_3 - X_1) - i\omega b_1(X_3 - X_2) - i\omega b_3 X_3. \tag{7c}$$

These expressions are further simplified by dividing all three Eqs. (7) by $m_1 = m_2$ and introducing the following notation:

$$\Omega^2 \equiv (k_1 + k_2)/m_1, \tag{8a}$$

$$\omega_1^2 \equiv k_2/m_1, \tag{8b}$$

$$\beta_1 \equiv b_1/m_1, \tag{8c}$$

$$\beta_3 \equiv b_3/m_1. \tag{8d}$$

Upon collecting the terms for each coordinate, the structure of the equations is more apparent:

$$A(\omega)X_1 - D(\omega)X_3 = F_1, \tag{9a}$$

$$A(\omega)X_2 - D(\omega)X_3 = F_2, \tag{9b}$$

$$D(\omega)(X_1 + X_2) = B(\omega)X_3, \tag{9c}$$

where

$$A(\omega) \equiv \Omega^2 - \omega^2 + i\beta_1\omega, \tag{9d}$$

$$B(\omega) \equiv 2\omega_1^2 - (m_3/m_1)\omega^2 + i\omega(2\beta_1 + \beta_3), \tag{9e}$$

$$D(\omega) \equiv \omega_1^2 + i\beta_1\omega, \tag{9f}$$

are complex coefficients.

Next Eqs. (9a), (9b), and (9c) are solved for the coordinates as a function of the external forces F_1 and F_2. The solutions are, using the gain $a \equiv V_2/V_1 = F_2/F_1$ and omitting the frequency dependence of the coefficients to simplify notation:

$$\frac{X_1}{F_1} = \frac{(AB - D^2) + aD^2}{A(AB - 2D^2)}, \tag{10a}$$

$$\frac{X_2}{F_1} = \frac{(AB - D^2)a + D^2}{A(AB - 2D^2)}, \tag{10b}$$

$$\frac{X_3}{F_1} = \frac{(1 + a)D}{AB - 2D^2}. \tag{10c}$$

Equation (10c) is proportional to an explicit expression for the shear rate in terms of the applied voltages. The other two will prove useful in obtaining an approximate expression for the friction coefficient.

By adding Eqs. (9a) and (9b), and dividing by (9a), one has:

$$1 + a = \frac{A(X_1 + X_2) - 2DX_3}{AX_1 - DX_3}. \tag{11}$$

Or, substituting Eq. (9c) into the numerator of this expression:

$$1 + a = \frac{(AB - 2D^2)X_3}{D(AX_1 - DX_3)}. \tag{12}$$

It is clear that if X_1 could be eliminated in favor of X_3 in the denominator, the unknown coordinates would completely cancel. Since there are not enough equations to do this exactly, an approximation must be made. It will be shown that if the system is sufficiently far from resonance, $|X_2| \ll |X_1|$ so that, to lowest order, Eq. (9c) becomes:

$$B(\omega)X_3 \approx D(\omega)X_1. \tag{13}$$

This may be inserted into Eq. (12) to obtain, finally:

$$a \approx D^2/(D^2 - AB). \tag{14}$$

To justify the approximation used in obtaining Eq. (14), consider the relative magnitudes of the coefficients $A(\omega)$, $B(\omega)$, and $D(\omega)$ in Eqs. (9d), (9e), and (9f). At suitably low frequencies ($\omega \ll \Omega$) it is clear from the fact that $\Omega^2 \gg \omega_1^2$ that $|A(\omega)| \gg |D(\omega)|$ and that while $|B(\omega)|$ and $|D(\omega)|$ may be of comparable magnitude, $|B(\omega)|$ is in any event greater than $|D(\omega)|$. Thus, Eqs. (10a) and (10b) give:

$$\frac{|X_2|}{|X_1|} = \frac{|(AB - D^2)a + D^2|}{|(AB - D^2) + aD^2|}. \tag{15}$$

And now, given the empirical fact that $|a| \ll 1$ except very near a resonance, a limit can be set on the magnitude of $|X_2|$:

$$\frac{|X_2|}{|X_1|} \sim \frac{|D^2|}{|AB - D^2|} \sim \frac{|D|}{|A|} \ll 1, \tag{16}$$

which justifies the approximation stated in Eq. (13). Starting with Eq. (14) it is possible to derive separate expressions for the magnitude of the gain, $|a|$, and the phase ϕ, which is the phase shift between the input and output voltages. The results are compared to the data in Figs. 7 and 8.

In Fig. 7(a) is displayed $|a|$ vs ω, with the solid line depicting the prediction of Eq. (14), and the circles actual calibrations taken from the device. To obtain this prediction, the values of the parameters appearing in Eq. (14) were varied to fit the data [these values are specified in the legend to Fig. 7(a)]. The parameters thus determined are quantitatively reasonable in view of the known mechanical properties of the separate device components.

There are two regions in which the predicted curve deviates from the observed form: near the resonance at $\omega \approx 300$ Hz, and in the very low frequency range [see the

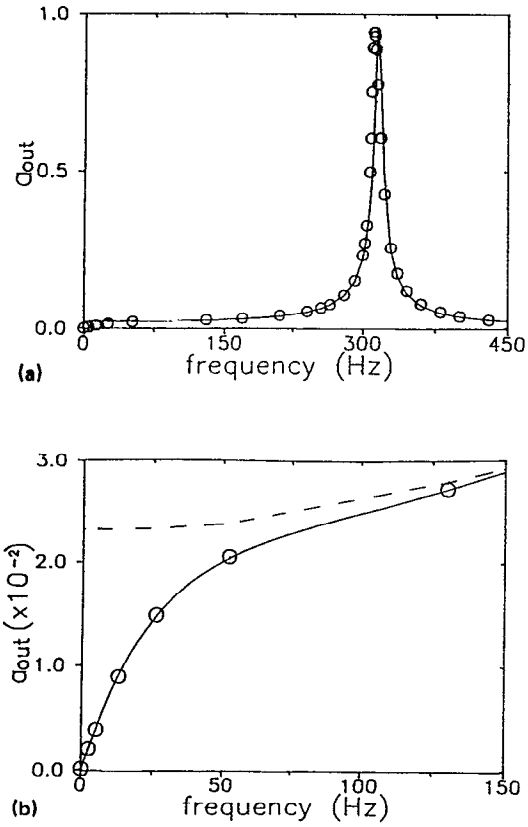

FIG. 7. (a) Gain as a function of frequency as determined by calibration (circles) and by the mechanical model (solid line). The model parameters used to give this fit are: $m_1 = m_2 = 0.721$g, $m_3 = 4.45$g, $k_1 = 1.90 \times 10^5$ N/m, $k_2 = 9.00 \times 10^3$ N/m, $b_1 = 0.113$ Ns/m, $b_3 = 0.00$ Ns/m (mica surfaces not touching). The deviations of the model from the data in the low frequency range [see also (b)] are due to electrical effects which are ignored in the mechanical model. (b) Gain vs. frequency in the low frequency range, as determined by calibration (circles), the mechanical model (dashed line), and the mechanical model corrected by the inclusion of the electrical model (solid line). The time constant RC is 0.014 seconds, determined by fit to the data. All other parameters have the same values as those used to generate 7(a).

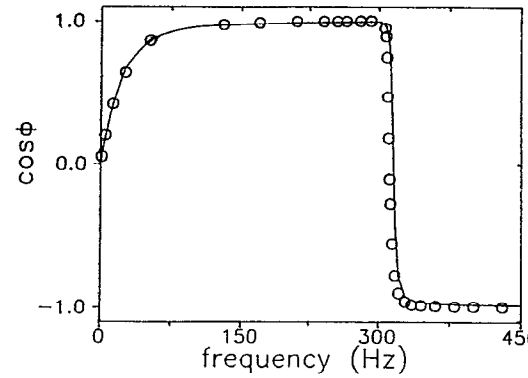

FIG. 8. The cosine of the phase lag ϕ between the input voltage and output voltage, with the surfaces not in contact, as a function of frequency. Data points are indicated by circles, and the results of the mechanical model corrected with the electrical model are shown as a solid line. The values of the parameters are the same as those used to generate Fig. 7(b).

dashed line in Fig. 7(b)]. In the former case, it is not surprising that there are deviations, since the approximations used to obtain Eq. (14) are not strictly speaking valid near to resonance. Considering this fact, the qualitative agreement is still quite good.

The reason for deviations at low frequencies is that, in the mechanical model, electronic effects arising from the process of data taking are ignored. Above it was implicitly assumed that the transduction voltages V_1 and V_2, which appear in the mechanical model, are identically the same as the applied and measured voltages, respectively. In fact, the presence of the instruments used to generate and measure voltages must be taken into account. This is the purpose of the electrical model.

IV. THE ELECTRICAL MODEL

The point of view in the development of the mechanical model is internal to the device; the transduction voltages V_1 and V_2, (and hence the forces f_1 and f_2), are assumed to be external influences whose values are specified, and the internal response of the device is then calculated. In the electrical model, the viewpoint is external to the device. The concern is not with what occurs within the apparatus, but rather how the apparatus interacts with the external control and measurement devices. From this perspective, the apparatus is a "black box" with two terminals, each of which participates in one of two circuits. These two circuits, the input and the output circuits, are electrically isolated from each other. The connection between them is made mechanically, and described by the mechanical model, as illustrated in Fig. 9(a). The goal of the electrical model is to determine the effective electrical components appearing in the input and output circuits.

From the point of view of circuit analysis, a bimorph is similar to a capacitor; it consists of two conducting plates with a dielectric between them. A bimorph differs from a capacitor, however, in that the presence of a stress or strain can effectively create an additional voltage source or voltage drop. Thus a bimorph is modeled electrically as a capacitor, together with one or more other electrical components to simulate the piezoelectric transduction. The exact configuration of components depends on how the bimorph is being used; the sender and receiver bimorphs behave differently, so they will be considered one at a time.

The model for the input circuit, which consists of the sender bimorph connected to the signal generator, will be derived first. In the absence of piezoelectric transduction, the sender bimorph would be equivalent to a normal capacitor (C). The voltage across this capacitor would then be the voltage (V) produced by the signal generator. When transduction is included, the dielectric constant of the capacitor, and hence the effective capacitance (C), changes as a function of time due to the conversion of some of the energy in the capacitor into mechanical energy. However, this does not alter the voltage across the effective capacitor, which is still determined by the signal generator. The energy loss due to transduction may thus be represented by

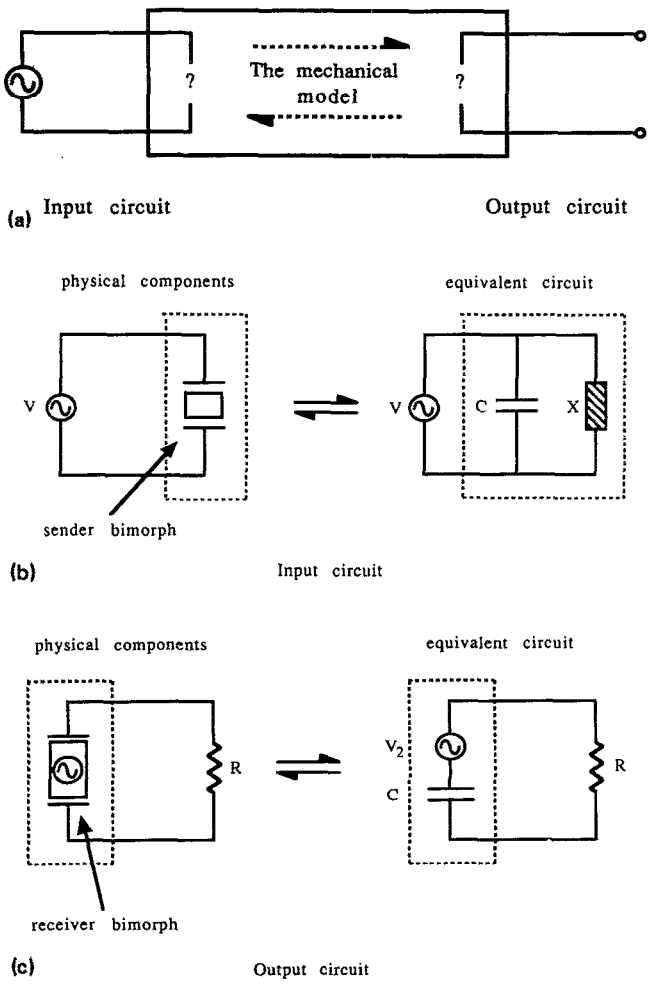

FIG. 9. (a) From the point of view of the electronics, the shear apparatus appears as two electrically isolated circuits. The connection between the two circuits is made mechanically, through the device, and described with the mechanical model. Understanding the purely electrical response of the shear device to the measurement and control devices requires the determination of the effective electrical components in the input and output circuits. (b) In the input circuit, the voltage across the sender bimorph is determined by the signal generator. The bimorph responds like a capacitor in parallel with another impedance representing the presence of piezoelectric transduction; consequently the force induced is proportional to this voltage V. (c) In the output circuit, the source of the signal V_2 is internal to the bimorph, being determined by the mechanical response of the device. This source charges the plates of the receiver bimorph, which in turn sets up a current in the measurement resistor R. The quantity V_2, which is the output voltage in the mechanical model, is thus not the same as the measured voltage across the resistor R, and a correction to the mechanical model must be applied.

including another impedance (X) in parallel with the capacitor [see Fig. 9(b)]. The exact nature of this impedance (X) is not of relevance. The point is that the voltage across this impedance (X) is the quantity V_1 referred to in the mechanical model, and since the impedance (X) is in parallel with the capacitor (C), it is obvious that $V_1 = V$. Hence no modification to the results of the mechanical model is required due to electronic effects in the input circuit.

The output circuit is not so straightforward to analyze, nor is the resulting correction so trivial. This circuit consists of the receiver bimorph connected to the detection device used to measure the output signal. The detection device has some large but finite input resistance (R). The quantity that is measured experimentally is the voltage across this resistor, (V_R). Once again, the starting point for a model is to introduce an effective capacitance (C). The voltage arising from the motion of the receiver bimorph appears as a source in the output circuit. The quantity V_2 in the mechanical model is the voltage produced by this source. Unlike the extra component in the input circuit, the source appears in *series* with the effective capacitance (C), not in parallel. This is evident from the physical origin of currents in the output circuit. The current in the resistor is caused by variations in the charge on the bimorph plates, which in turn arise because of piezoelectric transduction *within* the bimorph. The point is that the measurement device does not measure the transduction voltage source (V_2) directly, but rather the sum of this voltage and the voltage across the effective capacitor. This argument is shown pictorially in Fig. 9(c).

Because the measured voltage (V_R) is not the same as the transduction voltage (V_2), a correction must be applied to the mechanical model to compare it to the data. Using Ohm's law with the complex impedances in the equivalent circuit of Fig. 9(c), a relationship between V_R and V_2 can be obtained. In terms of the output current (I), total impedance of the circuit (Z) and the quantities introduced above, the result is

$$V_R = IR = \frac{V_2}{Z} R = V_2 \frac{R}{R + (1/i\omega C)} = V_2 \frac{\omega}{\omega + (1/iRC)}, \tag{17}$$

where $i \equiv \sqrt[2]{-1}$, and ω is the frequency. Combining this result with Eq. (14) yields the following prediction for the measured gain $a_{\text{obs}} \equiv V_R/V_1$:

$$a_{\text{obs}} \approx \frac{D^2}{(D^2 - AB)} \frac{\omega}{[\omega + (iRC)^{-1}]}. \tag{18}$$

The result of this correction is shown as the solid line in Fig. 7(b). The agreement is now excellent at low frequency. Using the same values for all the parameters, the prediction for the cosine of the phase lag ϕ is equally good, as shown in Fig. 8.

V. DETERMINATION OF THE APPARENT DYNAMIC VISCOSITY AND SHEAR RATE

So far this article has been concerned with the particulars of the model and establishing an understanding of how the device behaves. Next the results are applied to the determination of the apparent dynamic viscosity of the liquid layer under study. Within our model, the viscous friction of the liquid appears as a force acting on the boat [Eq. (4)]. In the final form for the gain (a) in Eq. (14), this force appears in the term $i\beta_3\omega$ in the coefficient $B(\omega)$. The other coefficients, $A(\omega)$ and $D(\omega)$, are independent of the friction of the liquid, and depend only upon frequency and the characteristics of the device itself. Thus, if the gain a_{out} when the surfaces are not in contact (and hence

$\beta_3 = 0$) is compared to the gain a_{in} when the surfaces are in contact, the following is obtained:

$$\frac{a_{out}}{a_{in}} = \frac{AB_{in} - D^2}{AB_{out} - D^2}, \tag{19}$$

where

$$B_{out}(\omega) \equiv 2\omega_1^2 - (m_3/m_1)\omega^2 + i\omega(2\beta_1 + \beta_3)$$

and

$$B_{in}(\omega) \equiv B_{out}(\omega) + i\beta_3\omega.$$

Note that the electrical correction shown in Eq. (17) has divided out.

Next, in order to simplify this result, we restrict ourselves to low frequencies ($\omega < \omega_{res}/10 \sim 30$ Hz). It is easy to expand the numerator and denominator, and keeping terms of lowest order in ω one can write:

$$\frac{a_{out}}{a_{in}} - 1 \approx \frac{i\omega\beta_3\Omega^2}{\omega_1^2(2\Omega^2 - \omega_1^2)}, \tag{20}$$

which can be restated in terms of more "physical" parameters using the definitions of the relevant parameters [Eqs. (8)]:

$$\frac{a_{out}}{a_{in}} - 1 \frac{i\omega m_1\beta_3(k_1 + k_2)}{k_2(2k_1 - k_2)} \approx \frac{i\omega b_3}{K}, \tag{21}$$

where $K \equiv 2k_1k_2/(k_1 + k_2)$ is the effective spring constant of the device as a whole, and is discussed in detail in the section pertaining to calibrations. Equating the imaginary parts of both sides results in the desired relationship between the gains and the friction coefficient:

$$\frac{|a_{out}|}{|a_{in}|}\sin(\phi) = \frac{\omega b_3}{K} \tag{22}$$

or, finally:

$$b_3 = \frac{K\sin(\phi)}{\omega}\frac{|a_{out}|}{|a_{in}|}, \tag{23}$$

where ϕ is the amount by which the in-contact signal lags the out-of-contact signal. This expression agrees with the spirit of the Massa and Shrag result, which pertains to dynamic oscillatory measurements on bulk polymer solutions.[15] Our quantity $|a_{out}|/|a_{in}|$ is analogous to their F_0/x_0, and in Eq. (23) the intrinsic friction of the device is already calibrated out and is thus not subtracted. In continuum hydrodynamics the coefficient b_3 is related to the apparent viscosity of the liquid by the relation[16]

$$\eta = hb_3/A, \tag{24}$$

where h is the thickness of the film and A is the area of contact.

The instantaneous shear rate $\dot{\gamma}$ is defined to be the velocity of shear divided by the film thickness. Since the driving force is sinusoidal, the instantaneous shear rate changes constantly throughout each cycle. The term "shear rate" will be used hereafter to mean the *magnitude* of the shear rate, $|\dot{\gamma}|$. For sinusoidal motion at a single frequency, ω, the shear rate is related to the magnitude of the displacement $|X_3|$ by

$$|\dot{\gamma}| \equiv |\omega X_3|/h. \tag{25}$$

Using this and Eq. (10c), the following form for the shear rate is obtained:

$$|\dot{\gamma}| = \frac{|\omega(1 + a)DF_1|}{h|AB - 2D^2|}. \tag{26}$$

Except near resonance, the quantity $|AB - 2D^2|$ is not noticeably different from $|AB - D^2|$ due to the fact that $k_1 \gg k_2$. Thus, it is safe to use the approximate expression, valid throughout the operating regime of the device:

$$\frac{|D|}{|AB - 2D^2|} \approx \frac{|D|}{|AB - D^2|} \approx \frac{|a|}{|D|}, \tag{27}$$

so that if terms of order $|a|^2$ are ignored in the numerator of Eq. (26), an expression for $|\dot{\gamma}|$ as a function of V_2 (the *output* voltage) is obtained:

$$|\dot{\gamma}| \frac{|\omega aF_1|}{|hD|} = \frac{\omega\Gamma|V_2|}{m_1h|D|} = \frac{\omega\Gamma|V_2|}{h|k_2 + ib_1\omega|}, \tag{28}$$

where the definition of $D(\omega)$ in Eq. (9f) has been used, and Γ is defined by $m_1F_1e^{i\omega t} \equiv f_1(t) \equiv \Gamma V_1(t)$, and represents the transduction efficiency (i.e., Newtons obtained per volt) of the bimorphs [see Eqs. (2) and (6b)]. To obtain an expression for $|\dot{\gamma}|$ in terms of the voltage which is actually measured, V_R, the electrical correction of Eq. (17) must be applied to Eq. (26). The result is

$$|\dot{\gamma}| \approx \frac{\Gamma|[\omega + (1/iRC)(V_R)|}{h|k_2 + ib_1\omega|}. \tag{29}$$

VI. VISCOELASTIC LIQUIDS

The mechanical model of the shear device developed above is readily generalized to permit the analysis of shear experiments performed on viscoelastic liquids. The elastic response can be included in the mechanical model by making the apparent dynamic viscosity, η, a complex quantity, η^*. The imaginary part of η^* is proportional to the elastic modulus, G', while the real part of η^* is just η, the apparent dynamic viscosity (which can be related to the loss modulus G''). In terms of the quantities in the mechanical model, the only change necessary is to replace b_3 with $b_3^* \equiv b_3 + ib_3'$. This in turn will transform the quantity $B_{in}(\omega)$ appearing in Eq. (19) into the quantity $B_{in}^*(\omega)$:

$$B_{in}^*(\omega) \equiv B_{out}(\omega) + i\beta_3^*\omega \equiv B_{out}(\omega) + i\beta_3\omega - \beta_3'\omega, \tag{30}$$

where $\beta_3^* \equiv b_3^*/m_1$, $\beta_3' \equiv b_3'/m_1$, and $B_{out}(\omega) \equiv 2\omega_1^2 - \omega^2 + i2\beta_1\omega$. This will not modify the determination of the real part of the friction coefficient derived previously [see Eq. (23)], but will permit the elastic part of the friction coefficient, b_3', to be determined from the following expression, which is valid to first order in ω:

$$b_3' = \frac{K}{\omega}\left(1 - \frac{|a_{out}|}{|a_{in}|}\cos(\phi)\right). \tag{31}$$

This expression is obtained by replacing β_3 with the quantity β_3^* in Eq. (21), and taking the real part of both sides. Depending on the magnitude of b_3', it may be necessary to keep terms of order ω^2 or even higher in the expansion of Eq. (19). However, given the extent to which the apparent viscosities of thin films are enhanced over their bulk values, it is possible that thin, viscoelastic films may have very large elastic moduli, so Eq. (31) may require no modification.

VII. CALIBRATION

The major results of the model in Eqs. (23) and (29) contain several device-specific parameters that must be determined by calibrations. In the expression for the friction coefficient [Eq. (23)], it is pleasing to note that the force-voltage constant Γ and the electrical correction factor derived in Eq. (17) divide out when the ratio of $a_{\text{out}}/a_{\text{in}}$ is taken, since these parameters are the same whether or not the surfaces are in contact. The only parameter which remains and must be determined by calibration is the effective spring constant of the device K. The determination of K is easy and will be discussed below.

The expression for the shear rate [Eq. (29)] unfortunately involves several parameters that do not divide out. Although in principle separate calibrations might be performed to determine each of these parameters independently, in practice, an easier approach is possible. Using the expressions for the shear rate given by Eqs. (25) and (29), the following expression for the maximum displacement of the boat can be obtained:

$$|X_3| = g(\omega)\,|V_R|, \tag{32}$$

where

$$g(\omega) \equiv \frac{|\omega + 1/iRC|\,\Gamma}{\omega\,|k_2 + ib_1\omega|}. \tag{33}$$

Since the goal is essentially to determine the value of $|\dot{\gamma}|$ as a function of $|V_R|$ and ω, it is simpler and more accurate to perform a single calibration to determine empirically the quantity $g(\omega)$, than to perform separate calibrations for each of the parameters contained in $g(\omega)$. Once $g(\omega)$ is known, the shear rate $|\dot{\gamma}|$ can be found from:

$$|\dot{\gamma}| = [\omega g(\omega)/h]\,|V_R|. \tag{34}$$

Experimentally, $g(\omega)$ is found to vary with ω in a manner consistent with this formula given the relative magnitudes of typical values of RC, k_2 and b_1 [see notes to Figs. 7(a) and 7(b)]. Thus the shear rate $|\dot{\gamma}|$ is approximately proportional to the output voltage $|V_2|$, with the coefficient being a (slowly varying) function of frequency.

The value of the device spring constant K is obtained from the inverse of the slope of a displacement versus force curve, such as that shown in Fig. 5. The reason for calling K the spring constant of the device is that applying a static force to the boat effectively displaces in parallel the two bimorph-leaf spring combinations, each of which is represented in the model as a series combination of two springs of constants k_1 and k_2. Hence, $K \equiv 2k_1k_2/(k_1 + k_2)$ is aptly named the spring constant of the device. In practice, K typically has values on the order of 10^3–10^4 Newtons per meter.

VIII. REGIMES OF OPERATION

There are several considerations that restrict the range of usable frequencies and input voltages of the device. Some are physical limitations of the apparatus and measurement techniques, others are restrictions on the validity of the model. In particular, physical characteristics of the device limit the maximum input voltage usable, while the highest frequency is limited by the validity of the model. There are also lower limits on both the frequency and voltage that arise from practical difficulties with the electrical measurement of very small and slowly varying signals. All of these restrictions, the limits they place on the shear rate, and some means of overcoming them, are discussed in detail below.

The expression derived for the friction coefficient of the liquid layer, Eq. (23), is an expansion of Eq. (19) to first order in ω, which limits the use of this expression to "low frequencies." If the expansion is continued to higher powers of ω, it is evident that the real parts of the expansion contain even powers of ω only, while the imaginary parts contain just the odd powers. Therefore, the first correction to Eq. (23) is proportional to ω^3, not ω^2, so one expects Eq. (23) to hold for $\omega < \omega_{\text{res}}/5$, where the resonance frequency, ω_{res}, is generally of order 300 Hz. This upper bound does not greatly restrict the range of attainable shear rates. Nevertheless, if required, the upper limit of usable frequencies could be extended by calculating the coefficient for the third order term. This coefficient involves new unknown parameters, whose determination would require the development of new calibrations.

The upper limit of usable input voltage arises because at high enough input voltages the response of the device ceases to be linear. Calibrations of dc input voltage versus displacement, such as the one shown in Fig. 4, typically exhibit linear response up through voltages on the order of 250–300 V. At nonzero frequencies under 500 Hz, however, the limiting voltage becomes lower, generally reaching its lowest value of 80 to 100 V at roughly 100 Hz, depending on the device. This cutoff, like the high-frequency limit, does not greatly restrict the operating range of the device.

More serious restrictions limit the use of low voltages and very low frequencies. The lower limit on input voltage arises from the fact that, at normal operating frequencies (frequencies less than 60 Hz), the device is far from resonance, and hence mechanically very inefficient. Input voltages much less than 100 mV result in output signals too small to measure, except by "signal averaging" them over many periods of oscillation.

This problem of small output signals is compounded at frequencies less than 10 Hz by the electrical attenuation explainable with the electrical model [see Eq. (17)]. At frequencies less than 0.5 Hz two additional problems arise. First, the rate of data taking becomes very slow, particularly when signal averaging is required. This is a difficulty

due to the danger of eventual contamination of the mica surfaces. Second, the time scale of the motions is sufficiently long that the device becomes sensitive to thermal drifts and random vibrations.

Despite all the limitations detailed above, the device has a large and useful operating range, being capable of shear rates between 10^{-1} and 10^{5} s^{-1}.

IX. DISCUSSION AND FUTURE PROSPECTS

In this article, we have endeavored to describe and characterize an apparatus developed for the study of the shear resistance of liquids in molecularly thin films. A model of the device developed to this end contains sufficient detail to understand thoroughly the behavior of the device and permit quantitative analysis of data collected. More than this, however, the model provides a starting point for the extension of the device to a broader regime of operations, and to the study of other physical systems. In particular, we have considered above the potential use of the shear device in studies of the mechanical response of viscoelastic liquids.

A benefit of the approach taken is that the meaning of the central quantity that emerges from the calculation is clear: the friction coefficient, b_3, of the thin liquid layer describes a physical force exerted on the apparatus by the liquid layer. It is a sensible quantity to define because the device is known to respond linearly to the applied voltage. This friction coefficient is reinterpreted as an apparent dynamic viscosity to facilitate comparison of thin film behavior with that of the bulk liquid. The central results of the analysis are quite general, however, and may be interpreted in different ways by rational extension as our understanding of these varied and exciting phenomena increases.

ACKNOWLEDGMENTS

We acknowledge the support of the National Science Foundation through the Materials Research Laboratory at the University of Illinois, Urbana-Champaign, Grant No. NSF-DMR-89-20538. J. Van Alsten acknowledges support from Grant No. NSF-MSM-88-19796.

APPENDIX: ON THE COMPLIANCE OF THE ADHESIVE

It has been assumed throughout the body of the text, and particularly in the development of the model, that the adhesive used to bind the mica sheets to the lenses is sufficiently compliant that the surfaces can be caused to flatten, yet sufficiently stiff that it does not influence measurements of the viscosity. It is easily verified that the surfaces do flatten (when properly induced) from the shape of the interference fringes observed. That the adhesive is stiff enough not to affect the measurements is not so easily verified, and requires some discussion.

Two mica surfaces brought together in dry air are said to be in "hard," or "adhesive" contact. On the scale of forces relevant in the shear experiments described above, mica surfaces in adhesive contact stick together so well that they may be considered rigidly attached. Accordingly, if an input voltage is applied to the device when the surfaces are in hard contact, the output waveform reflects in the main the response of the adhesive used to mount the surfaces. With the adhesives normally used, output signals observed with the surfaces in hard contact are found to be attenuated by 80% or more relative to output signals obtained with the surfaces out of contact. This shows that the adhesive's mechanical impedance is an order of magnitude larger than that of the device.

In contrast, the dynamic response of a liquid layer is only very slightly attenuated relative to the response observed with the surfaces out of contact. This shows that the mechanical impedance of the liquid is much smaller than that of the adhesive. Thus, the motion being observed in the measurements is not in the main the motion of the adhesive, except when one observes the yield stress behavior like that shown in Fig. 2(b).

[1] G. Carson and S. Granick, J. Mater. Res. **5**, 1745 (1990).
[2] C. Kessel and S. Granick, Langmuir (in press).
[3] J. Van Alsten and S. Granick, Phys. Rev. Lett. **61**, 2570 (1988).
[4] J. Van Alsten and S. Granick, Tribol. Trans. **32**, 246 (1989).
[5] J. Van Alsten and S. Granick, Mater. Res. Soc. Proc. **140**, 125 (1989).
[6] J. Van Alsten and S. Granick, Mater. Res. Soc. Proc. **153**, 317 (1989).
[7] J. Van Alsten and S. Granick, Langmuir **6**, 876 (1990).
[8] J. Van Alsten and S. Granick, Macromol. **23**, 4856 (1990).
[9] S. Granick, Science (in press).
[10] J. N. Israelachvili and G. E. Adams, J. Chem. Soc. Faraday Trans. **74**, 975 (1978).
[11] J. N. Israelachvili and P. M. McGuiggan, Science **241**, 795 (1988).
[12] J. N. Israelachvili, J. Coll. Interface Sci. **44**, 259 (1973).
[13] C. Luesse, J. Van Alsten, G. Carson, and S. Granick, Rev. Sci. Instrum. **59**, 811 (1988).
[14] W. P. Mason, *Electro-Mechanical Transducers and Wave Filters*, 2nd ed. (Van Nostrand, New York, 1948), pp. 200–217
[15] D. J. Massa and J. L. Schrag, J. Polym. Sci. A-2 **10**, 71 (1972).
[16] L. D. Landau and E. M. Lifshitz, *Fluid Mechanics* (Pergamon, Oxford, 1987).